

THE SUBLUMINOUS TYPE IA SUPERNOVA 1998DE IN NGC 252

MARYAM MODJAZ¹, WEIDONG LI², ALEXEI V. FILIPPENKO², JENNIFER Y. KING¹, DOUGLAS C. LEONARD², THOMAS MATHESON², AND RICHARD R. TREFFERS²

Department of Astronomy, University of California, Berkeley, CA 94720-3411

Submitted to PASP 2000 July 29

ABSTRACT

We present spectroscopic and extensive photometric observations of supernova (SN) 1998de in the S0 galaxy NGC 252, discovered during the course of the Lick Observatory Supernova Search. These data, which span a time period of 8 days before to 76 days after *B*-band maximum, unambiguously establish SN 1998de as a peculiar and subluminous type Ia supernova (SN Ia) with strong similarities to SN 1991bg, the prototype of these intrinsically dim SNe Ia. We find that SN 1998de, which has $\Delta m_{15}(B) = 1.96 \pm 0.09$ mag, rises and declines much faster than normal SNe Ia and does not exhibit the usual plateau in the *R* band. In the *I* band it shows a short plateau phase or possibly a secondary maximum, soon after the first maximum. We find that subluminous SNe with the same value of $\Delta m_{15}(B)$ can have slightly different light curves at longer wavelengths. The notable spectroscopic similarities between SN 1998de and SN 1991bg are the wide Ti II trough at 4100–4500 Å, the strong Ca II features, and the early onset of the nebular phase. We observe that spectroscopic deviations of SN 1998de from SN 1991bg increase toward redder wavelengths. These deviations include the absence of the conspicuous Na I D absorption found in SN 1991bg at 5700 Å, and the evolution of a region (6800–7600 Å) from featureless to feature-rich. Several lines of evidence suggest that SN 1998de was a slightly more powerful explosion than SN 1991bg. We discuss the implications of our observations for progenitor models and the explosion mechanism of peculiar, subluminous SNe Ia.

Subject headings: supernovae: general — supernovae: individual (SN 1998de, SN 1991bg)

1. INTRODUCTION

Supernovae (SNe) are classified into two main categories according to whether there are hydrogen lines present in their spectrum, usually taken near peak brightness: hydrogen-deficient supernovae are designated as Type I (SNe I), while those with hydrogen are Type II (SNe II). The category of SNe I is again subdivided into SNe Ia, Ib, or Ic, depending on whether they show further spectral features. Type Ia supernovae (SNe Ia) are identified by the appearance of a strong absorption feature at about 6150 Å due to blueshifted Si II $\lambda 6355$ (see, e.g., Filippenko 1997; Harkness & Wheeler 1990 for reviews).

A striking feature of SNe Ia has been their homogeneity; they have only moderate scatter in observed absolute peak magnitudes (Hamuy et al. 1996a) and similar light-curve shapes and spectra (e.g., Leibundgut & Pinto 1992; Branch & Tamman 1992; Filippenko 1997; Branch 1998). Moreover, the observed variations in luminosity among SNe Ia are found to be correlated with their light-curve shape, hence furnishing a tool to accurately calibrate the peak luminosity of SNe Ia (e.g., the $\Delta m_{15}(B)$ method — Phillips 1993, Hamuy et al. 1999a,b; Phillips et al. 1999; the multi-color light-curve shape method — Riess, Press, & Kirshner 1996, Riess et al. 1998a; the stretch method — Perlmutter et al. 1997). This has led to the successful usage of SNe Ia as “calibrated candles” for both nearby and cosmological distances, and in the context of an array of applications such as tracing the expansion history of the Universe (Riess et al. 1998a; Perlmutter et al. 1999), measuring the Hubble constant (e.g., Branch 1998; Jha

et al. 1999), studying the peculiar motions and bulk flows of galaxies (e.g., Riess, Press, & Kirshner 1995; Zehavi et al. 1998; Riess 1999), and probing the chemical evolution of galaxies (see, e.g., Pagel 1997 for a review).

In 1991, however, two nearby objects showed that there can occasionally be extreme deviants among SNe Ia: SN 1991bg, an intrinsically very dim SN Ia (Filippenko et al. 1992b, hereafter referred to as F92; Leibundgut et al. 1993, hereafter L93; Ruiz-Lapuente et al. 1993; Turatto et al. 1996, hereafter T96; Mazzali et al. 1997, hereafter M97), and SN 1991T (Filippenko et al. 1992a; Ruiz-Lapuente et al. 1992; Phillips et al. 1992; Jeffery et al. 1992), an intrinsically overluminous object. Both of these SNe showed clear spectral differences from typical SNe Ia. Over the last decade, more instances have been found which exhibit distinct photometric and spectroscopic peculiarities, and it is now commonly thought that this group of so-called “peculiar” SNe Ia can be subdivided into SN 1991bg-like (subluminous) objects and SN 1991T-like (overluminous) objects. Although Branch, Fisher, & Nugent (1993) found that approximately 85% of all previously observed SNe Ia were normal (“Branch-normal”), recent results by Li et al. (2000b,c,d) suggest an intrinsic peculiarity rate of as high as 36% (20% SN 1991T-like, 16% SN 1991bg-like).

Whereas many normal SNe Ia have been studied in detail and well-sampled light curves have been published, only a few peculiar SNe Ia (specifically of the subluminous variety) have been thoroughly observed. Examples include SN 1991bg, SN 1992K (Hamuy et al. 1994), and SN 1997cn

¹modjaz, jyking@ugastro.berkeley.edu

²wli, alex, dleonard, tmatheson, rtreffers@astro.berkeley.edu

(Turatto et al. 1998). A detailed study is necessary to address concerns about the utility of peculiar SNe Ia as reliable distance indicators, as well as to answer questions about their progenitor systems and explosion mechanisms.

In this paper we present SN 1998de as another instance of a peculiar, subluminous SN Ia. It was the eighth SN discovered by the Lick Observatory Supernova Search (LOSS; Treffers et al. 1997; Li et al. 2000a; Filippenko et al. 2000) with the 0.75-m Katzman Automatic Imaging Telescope (KAIT; Richmond, Treffers, & Filippenko 1993; Filippenko et al. 2000). A description of the observations and analysis, including our methods of performing photometry, our calibration of the measurements onto the standard Johnson-Cousins system, our resulting multi-color light curves, and our comparisons between the light curves of SN 1998de, SN 1991bg, and other SNe Ia is given in §2. The absolute magnitudes of SN 1998de are presented in §3. Section 4 contains a description of the observations and analysis of the spectra of SN 1998de, including a thorough comparison of the spectra of SN 1998de, SN 1991bg, and the normal SN Ia 1994D. We discuss the implications of our observations on constraining progenitor models in §5 and summarize our conclusions in §6.

2. PHOTOMETRY

2.1. Observations and Reductions

SN 1998de, located $72''$ from the nucleus of the S0 galaxy NGC 252, was discovered at $m \approx 18.4$ mag by Modjaz et al. (1998) in an unfiltered image obtained on 1998 July 23.5 and confirmed on July 24.5 during the LOSS.³ A KAIT image on July 19.5 already revealed a hint of the supernova, whereas a KAIT image on July 14.5 with a limiting magnitude of about 19 did not show any star at the supernova's position, $\alpha = 0^h48^m06^s.88$ and $\delta = +27^\circ37'28''.5$ (equinox J2000.0). Due to the search's small baseline (that is, the time interval to repeat observations of target galaxies; ~ 3 to 5 days), this supernova was caught 8 days prior to maximum brightness (on 1998 July 31.6 in *B*, see §2.2). Garnavich et al. (1998) classified a spectrum of SN 1998de obtained on July 25.4 as Type Ia by the presence of a broad absorption feature of Si II at 6185 \AA , noting that Ti II absorption at the blue end of the spectrum and strong Si II at 5800 \AA suggested a peculiar and subluminous event, similar to SN 1991bg.

A KAIT monitoring program of broadband *BVRI* photometry was established for SN 1998de two days after discovery and it continued for about 2 months. Also, optical spectra of SN 1998de were obtained sporadically with the 3-m Shane reflector at Lick Observatory 1–2.5 months past maximum brightness. The photometric data were collected with the 512×512 pixel CCD camera (AP7) made by Apogee Instruments at the $f/8.2$ Cassegrain focus of KAIT with exposure times in the range of 300 (in *R* and *I*) and 600 seconds (in *B* and *V*). The scale was $0''.8$ per pixel and the field of view was $6'.7 \times 6'.7$. The typical seeing at Lick was between $2''$ and $3''$ full width at half maximum (FWHM). The bias and dark-current subtraction with subsequent twilight-sky flatfielding were accomplished automatically at the telescope. Significant

fringing in the *I* band could not be completely removed despite various attempts to do so, but this phenomenon has only a small impact on our results because the SN and comparison stars were considerably brighter than the background.

The telescope's autoguiding device failed between July 25 and July 28. Multiple 60-s exposures were taken in each filter during that time, since the tracking mechanism was sufficiently accurate for exposure times of $\lesssim 100$ s. They were later aligned and combined to form a single frame in each filter.

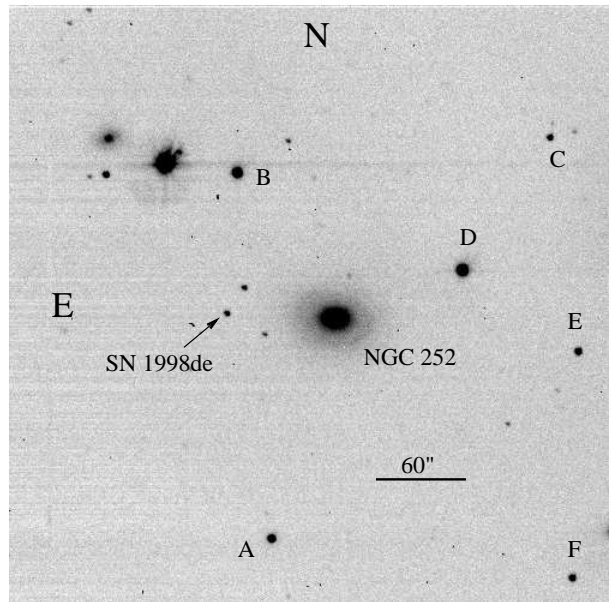


Figure 1. - V-band KAIT image of the field of SN 1998de, taken on 1998 July 31. The field of view is $6'.7$ by $6'.7$. The six local standard stars are marked (A–F), and SN 1998de is about $72''$ east and $3''$ north of the nucleus of NGC 252.

Figure 1 shows a KAIT V-band image taken on 1998 July 31 with SN 1998de and six comparison stars marked. Absolute calibration of the field was done on 1998 September 19, 20, and 21 by observing Landolt (1992) standard stars at different airmasses throughout the photometric nights. Instrumental magnitudes for the standards were measured by employing simple aperture photometry with the IRAF⁴ DAOPHOT package (Stetson 1987) and then used to determine transformation coefficients to the standard systems of Johnson (Johnson et al. 1966 for *BV*) and Cousins (Cousins 1981 for *RI*). The derived transformation coefficients and color terms were used to calibrate the sequence of six stars near SN 1998de that functioned as comparison stars for the supernova's brightness. The magnitudes of these six local standard stars and the associated uncertainties derived by averaging over the three photometric nights are listed in Table 1. Since the field of view between July 25 and July 28 did not include the local standards E and F, those stars were not used when computing the brightness of SN 1998de for those dates.

We implemented the point-spread-function (PSF) fitting technique for the differential photometry of the supernova relative to the comparison stars. Due to the fortunate

³We use UT dates throughout this paper.

⁴IRAF (Image Reduction and Analysis Facility) is distributed by the National Optical Astronomy Observatories, which are operated by the Association of Universities for Research in Astronomy, Inc., under cooperative agreement with the National Science Foundation.

TABLE 1
MAGNITUDES OF LOCAL STANDARD STARS

Star	B	σ_B	V	σ_V	R	σ_R	I	σ_I
A	15.701	0.005	14.860	0.003	14.390	0.001	13.996	0.007
B	14.462	0.009	13.708	0.003	13.268	0.003	12.916	0.003
C	17.460	0.010	16.541	0.004	16.012	0.007	15.520	0.011
D	13.736	0.005	13.092	0.003	12.733	0.003	12.443	0.003
E	16.346	0.003	15.652	0.004	15.267	0.008	14.971	0.006
F	16.486	0.006	15.727	0.003	15.315	0.010	14.988	0.011

position of the supernova far from the nucleus of the host galaxy in a region with a faint and smoothly varying background, measuring the brightness of the supernova was not hampered by a complex environment, which usually necessitates template subtraction (e.g., Filippenko et al. 1986; Richmond et al. 1995). We could have chosen simple aperture photometry as our technique, but we decided against it; besides giving more accurate photometry than apertures for objects projected upon slightly more complex regions (Schmidt et al. 1993), PSF fitting has the advantage of creating an image in which the measured objects are subtracted. This can serve as an indicator of the quality of the brightness measurements of the comparison stars and the supernova.

Before the photometry procedure itself was initiated, special care was taken to remove cosmic rays, especially those around the PSF stars. Since our particular CCD camera is cooled thermoelectrically rather than with liquid nitrogen (for mechanical simplicity, and to decrease human maintenance of the robotic telescope), the temperature of the camera is not very stable and dark current is not always cleanly removed from the images. The resulting low-level dark-current residual varies during the night and has to be removed manually by adding or subtracting a few percent of the long-exposure dark-current image. The uncertainties introduced by the manual scaling of the dark current have only negligible effects on the brightness measurement of the high-contrast SN and the PSF stars.

The PSF for each image was determined with DAOPHOT using well-isolated stars in the field, which are neither too bright (saturated) nor too faint. We only used the inner core of SN 1998de and the local standards to fit the PSF in order to increase the signal-to-noise (S/N) ratio. To measure the sky backgrounds of the SN and the local standards, we always used an annulus with an inner radius of 15 pixels ($12''$) and an outer radius of 20 pixels ($16''$).

The instrumental magnitudes measured from the PSF-fitting method were transformed onto the Johnson-Cousins system. Atmospheric extinction corrections were not considered since the net effect of this extinction is expressed through an additive constant that falls out when doing differential photometry. The linear transformations using the color terms derived from calibration observations on 1998 September 19, 20, and 21 were determined to be of the following form:

$$b = B - 0.086(B - V) + C_B,$$

$$\begin{aligned} v &= V + 0.029(B - V) + C_V, \\ r &= R - 0.151(V - R) + C_R, \\ i &= I - 0.057(V - I) + C_I. \end{aligned}$$

In the equations above, the upper-case passband letters signify magnitudes in the standard Johnson-Cousins system, whereas the lower-case letters denote instrumental magnitudes. The constants C_B , C_V , C_R , and C_I are the differences between the zero-points of the instrumental and standard magnitudes.

Since the search itself is conducted using unfiltered CCD observations for efficiency reasons (an unfiltered CCD image can reach fainter stars in less time than a filtered image), the magnitudes from the discovery and confirmation nights had to be transformed to a standard passband in order to compare with subsequent filtered observations. The employed method, which has also been used by Schmidt et al. (1998) and Riess et al. (1999), treats the unfiltered data as observations in the pseudo-passband ‘‘Clear’’ (C), so that the conversion equation into the standard passband B is simply expressed by the pseudo-color $B - C$. We chose to transform the unfiltered data to the standard passbands B and V (the former to follow the convention of measuring the light curves relative to B maximum and the latter because the V response curve is a closer match to the unfiltered response function). The results of detailed examinations by Riess et al. (1999) of the involved conversion parameters (e.g., the response function of KAIT’s CCD) yield a linear relation for stars between the standard color $B - V$ and the pseudo-color of the following form: $B - C = C_{BC}(B - V)$.

Here B and V are the standard Johnson passbands B and V , and C_{BC} is the slope of the linear relationship between the standard color $B - V$ and the pseudo-color $B - C$, empirically measured to be 1.33 ± 0.10 (Riess et al. 1999). Analogously, C_{VC} , the transformation coefficient to V , is measured to be 0.33 ± 0.10 .

Although the spectra of supernovae do not resemble those of normal stars (e.g., Filippenko 1997), their photometric behavior at very early times can be best approximated with a thermal model; see Riess et al. (1999) for a detailed discussion. Thus the transformation equations for the supernova (SN) and the local standards (LS) are $B_{SN} - C_{SN} = C_{BC}(B - V)_{SN}$, $B_{LS} - C_{LS} = C_{BC}(B - V)_{LS}$. Combining the two equations we can infer the standard B magnitude of the supernova,

TABLE 2
PHOTOMETRIC OBSERVATIONS OF SN 1998DE

UT Date DD/MM/YY	JD – 2,451,000.0	Phase ^a (days)	B (σ_B)	V (σ_V)	R (σ_R)	I (σ_I)
23/07/98 ^b	18.0	–8	19.42 (0.30)	18.62 (0.10)
24/07/98 ^b	19.0	–7	19.07 (0.20)	18.26 (0.08)
25/07/98	20.0	–6	...	17.79 (0.05)	17.53 (0.03)	17.67 (0.05)
26/07/98	21.0	–5	18.36 (0.06)	17.55 (0.03)	17.36 (0.03)	17.39 (0.05)
27/07/98	22.0	–4	...	17.36 (0.03)	17.08 (0.03)	17.12 (0.07)
28/07/98	23.0	–3	17.84 (0.04)	17.25 (0.03)	16.98 (0.02)	17.03 (0.06)
29/07/98	24.0	–2	17.73 (0.04)	17.08 (0.03)	16.89 (0.03)	16.94 (0.04)
30/07/98	25.0	–1	17.62 (0.04)	16.95 (0.02)	16.77 (0.03)	16.83 (0.03)
31/07/98	26.0	0	17.60 (0.03)	16.95 (0.03)	16.73 (0.03)	16.75 (0.04)
01/08/98	27.0	+1	17.63 (0.03)	16.87 (0.03)	16.62 (0.03)	16.67 (0.04)
02/08/98	28.0	+2	17.66 (0.02)	16.85 (0.02)	16.61 (0.03)	16.70 (0.03)
03/08/98	29.0	+3	17.77 (0.03)	16.83 (0.02)	16.63 (0.02)	16.63 (0.04)
04/08/98	30.0	+4	17.83 (0.03)	16.85 (0.03)	16.60 (0.02)	16.54 (0.03)
06/08/98	32.0	+6	18.14 (0.04)	17.01 (0.02)	16.73 (0.03)	16.69 (0.05)
07/08/98	33.0	+7	18.35 (0.06)	17.08 (0.02)	16.76 (0.03)	16.70 (0.04)
08/08/98	33.9	+8	18.54 (0.08)	17.17 (0.03)	16.82 (0.02)	16.68 (0.03)
09/08/98	34.9	+9	18.85 (0.08)	17.28 (0.03)	16.89 (0.02)	16.68 (0.03)
11/08/98 ^c	37.0	+11	...	17.45 (0.06)	16.98 (0.04)	16.69 (0.08)
12/08/98 ^c	38.0	+12	19.26 ^d (0.12)	17.57 (0.08)	17.10 (0.07)	...
13/08/98 ^c	39.0	+13	...	17.80 (0.08)	17.18 (0.05)	...
15/08/98	41.0	+15	19.54 (0.11)	17.92 (0.04)	17.32 (0.03)	16.94 (0.04)
16/08/98	41.8	+16	...	18.03 (0.04)	17.40 (0.03)	17.02 (0.04)
17/08/98	43.0	+17	19.71 ^d (0.06)	18.08 (0.04)	17.50 (0.03)	17.10 (0.04)
18/08/98	44.0	+18	...	18.25 (0.04)	17.61 (0.03)	17.17 (0.04)
19/08/98	44.8	+19	19.71 (0.07)	18.34 (0.04)	17.71 (0.04)	17.30 (0.05)
21/08/98	46.8	+21	19.91 (0.08)	18.53 (0.05)	17.89 (0.03)	17.48 (0.05)
23/08/98	48.9	+23	20.07 (0.11)	18.64 (0.06)	18.05 (0.03)	17.69 (0.04)
25/08/98	50.8	+25	20.02 (0.12)	18.70 (0.05)	18.22 (0.04)	17.75 (0.06)
27/08/98	52.8	+27	20.17 (0.17)	18.90 (0.06)	18.32 (0.04)	17.90 (0.05)
29/08/98	54.8	+29	20.25 (0.20)	19.03 (0.06)	18.48 (0.04)	18.07 (0.05)
31/08/98	56.8	+31	...	19.08 (0.09)	18.54 (0.05)	18.10 (0.07)
10/09/98	67.0	+41	...	19.36 (0.19)	18.98 (0.13)	18.84 (0.20)
15/09/98	71.8	+46	...	19.46 (0.07)	19.17 (0.05)	19.02 (0.14)
20/09/98 ^d	76.8	+51	20.88 (0.20)	19.63 (0.08)	19.41 (0.06)	19.16 (0.09)

^aRelative to the epoch of B maximum (JD=2,451,026.1).

^bOriginally clear observation.

^cBright full moon.

^dMeasured from combined images.

$$B_{SN} = B_{LS} - (C_{LS} - C_{SN}) - C_{BC}[(B-V)_{LS} - (B-V)_{SN}].$$

The amount of color evolution of the infant supernova, encapsulated by the term $(B-V)_{SN}$ for the discovery and confirmation observations, has a direct impact on our derived values for the standard magnitudes and cannot be directly measured, but rather has to be derived from later points. We chose the value of $(B-V)_{SN}$ on the dates of the unfiltered observations to be the same as on $t = -5$ days, since the color of a SN Ia seems to evolve slowly at early times, as indicated by Riess et al. (1999). Because the V band better matches the unfiltered CCD, a significant change in the $B-V$ color influences the data transformed to B more than those transformed to V . This explains the larger uncertainty in the B magnitude as compared to the one in V .

Table 2 shows our final results for all photometric observations ranging from 8 days prior to B maximum until 51 days after maximum brightness. Uncertainties were estimated by combining in quadrature the errors given by the error analysis package in DAOPHOT with those introduced by the transformation of instrumental magnitudes onto the standard system. Since SN 1998de was a relatively faint and red supernova, bad weather conditions influenced our data and affected the B images the most. For the sets of nights of August 11/12/13, August 16/17/18, and September 19/20/21, the B images had to be combined to yield one single image for each set in order to obtain a sufficiently high S/N ratio. The data for September 19/20/21, the last three nights of observation, were combined in this manner for all filters, since the SN was already very faint at that point. For the combined images, the epoch of the observation was taken to be August 12, August 17, and September 20, respectively.

2.2. Optical Light Curves

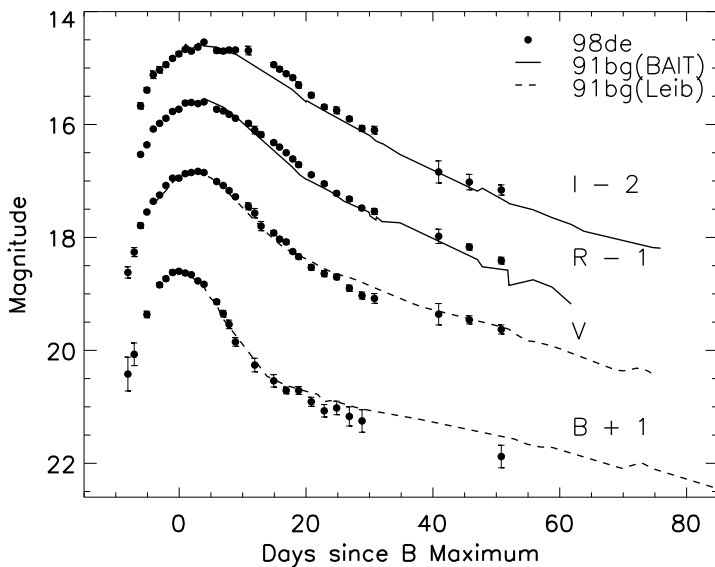


FIG. 2. - The B , V , R , and I light curves of SN 1998de, along with those of SN 1991bg (RI from F92: “BAIT”; BV from L93: “Leib”) which are shifted in times and peak magnitudes to match those of SN 1998de. The time zero-point is the date of maximum light in the B passband, here 1998 July 31 UT.

Figure 2 displays our $BVRI$ light curves of SN 1998de together with those of SN 1991bg (F92; L93). For all SN 1998de points except the marked ones, the uncertainties are smaller than the plotted symbols. Due to the proximity of the SN ($cz = 4950 \text{ km s}^{-1}$; see §3), we did not apply any redshift corrections (time dilation, K terms). The values for the date and the magnitude of the peak in each filter are given in Table 3; they were determined by fitting different spline functions and polynomials to the $BVRI$ light curves around maximum brightness. Since we have ample pre- and post-maximum data points, the uncertainties in our values are comparatively small, except in the I band ($\sigma_I = 1.1$ days), where there does not seem to be one clear peak. Here, and in all subsequent discussions and figures, the variable t denotes time since maximum brightness in the B passband (JD=2,451,026).

In Figures 3–6, we compare the light curves of SN 1998de with those of several other well-observed SNe Ia representing the diversity of SN Ia light curves: SN 1991T (Hamuy et al. 1996b for BVI ; Ford et al. 1993 for R) as an example of an overluminous SN Ia; SN 1989B (Wells et al. 1994) and SN 1994D (Richmond et al. 1995) as examples of normal SNe Ia, and SN 1991bg (F92 for RI ; L93 for BV) as the prototypical subluminal SN Ia. All light curves are shifted in time and peak magnitude to match those of SN 1998de with the time zero-point being the date of maximum light in the B passband. The data for the SN 1991bg-like objects SN 1992K (Hamuy et al. 1994) and SN 1997cn (Turatto et al. 1998) are not explicitly included here, since they are claimed to be twins to SN 1991bg both photometrically and spectroscopically, but comments and comparisons are provided.

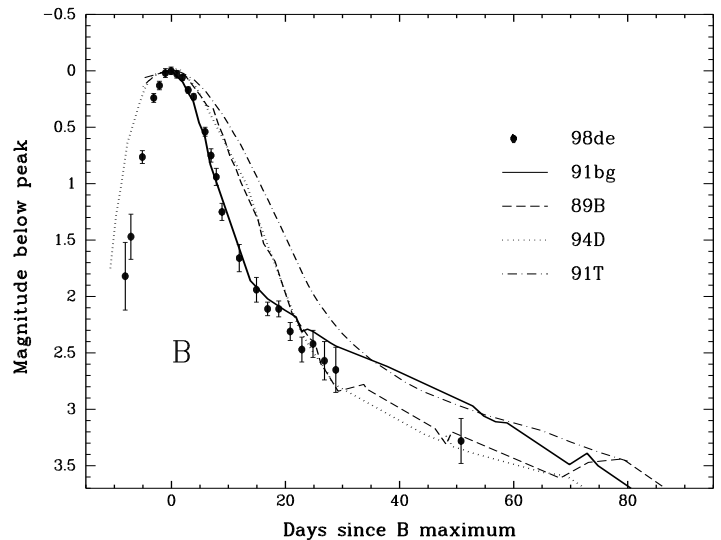


FIG. 3. - The B light curve of SN 1998de, together with those of SN 1991bg (L93), SN 1991T (Hamuy et al. 1996b), SN 1989B (Wells et al. 1994), and SN 1994D (Richmond et al. 1995). All light curves are shifted in times and peak magnitudes to match that of SN 1998de.

Figures 2–6 show unambiguously that the early-time light curves of SN 1998de closely resemble those of SN 1991bg. Nevertheless, there seems to be a certain trend, where the discrepancies may increase with increas-

TABLE 3
PHOTOMETRIC INFORMATION ON SN 1998DE

Filter	<i>B</i>	<i>V</i>	<i>R</i>	<i>I</i>
Epoch of max.	Jul. 31.6 ± 0.1	Aug. 3.1 ± 0.2	Aug. 3.3 ± 0.5	Aug. 4.2 ± 1.1
Julian Date of max. – 2,451,000.0	26.1 ± 0.1	28.6 ± 0.2	28.8 ± 0.5	29.7 ± 1.1
Magnitude at max.	17.60 ± 0.04	16.84 ± 0.04	16.62 ± 0.04	16.60 ± 0.05
Δm_{15}	1.96 ± 0.09	1.34 ± 0.06	1.02 ± 0.06	0.69 ± 0.09

ing wavelength of the passband so that the closest match between the two SNe is in the *B* passband (except at late times). On the other hand, the most notable similarities in all filters are the narrow peak, beautifully exhibited by SN 1998de, and the rapid decline rate distinguishing these two SNe from the rest of the sample. Here SN 1998de displays among the best premaximum observations in our chosen sample — only 1994D was caught at a comparably early time. Unlike the case for SN 1991bg, for which there were no premaximum observations (or only a few in *V*, see L93), our data clearly establish SN 1998de as a fast riser.

The *B*-band light curve of SN 1998de (Figure 3) matches that of SN 1991bg very closely at early times, but seems to decline faster at late times (for $t \gtrsim 20$ days). In accordance with Phillips (1993) and Hamuy et al. (1996a,b), we define $\Delta m_{15}(X)$ to be the decline (in magnitudes) during in the first 15 days after maximum brightness in the passband *X*, and we measure $\Delta m_{15}(B)=1.96 \pm 0.09$ for SN 1998de. The uncertainty is the sum in quadrature of the uncertainty in the *B*-band peak magnitude, the change in the interpolated magnitude 15 days after peak (if the date of maximum is changed by the amount listed in Table 3), and the uncertainty of the observed magnitudes. This Δm_{15} value is nearly identical to that of SN 1991bg [$\Delta m_{15}(B)=1.93$, Hamuy et al. 1996b; $\Delta m_{15}(B)=1.95$, T96], and constitutes the largest value in our comparison sample of SNe Ia [$\Delta m_{15}(B)=1.31$ for SN 1994D, Richmond et al. 1995; 0.94 for SN 1991T, Hamuy et al. 1996b; 1.31 for SN 1989B, Wells et al. 1994] and of all SNe sampled during the Calán/Tololo Supernova Survey (Hamuy et al. 1996a). Both SN 1998de and SN 1991bg reach the “knee” in the light curve, where the fast decline phase makes a transition to a slower decline phase, at $t \approx 14$ days. But the knee is more pronounced (and perhaps a bit earlier) in SN 1991bg than in SN 1998de; after that point, SN 1991bg fades at a rate of 0.029 ± 0.03 mag day⁻¹ (L93) and SN 1998de fades at ~ 0.048 mag day⁻¹. There seems to be a steadily growing deviation from the SN 1991bg curve at late times (for $t \gtrsim 20$ days), although the uncertainties of each individual measurement are relatively large. We can believe this deviation, since all data points of SN 1998de lie consistently below the SN 1991bg curve, and we conclude that it is due to an intrinsic difference between the photometric behavior of the two SNe at late times.

The *V*-band curve is shown in Figure 4, and reveals consistent similarities between SN 1998de and SN 1991bg, reinforcing the narrow-peak behavior. We measure $\Delta m_{15}(V)=1.34 \pm 0.06$, slightly smaller than the corre-

sponding value for SN 1991bg, $\Delta m_{15}(V)=1.42$ (L93). SN 1998de therefore declined a bit more slowly than SN 1991bg in the *V* band. The knee in the *V* band is reached at $t \approx 19$ days, rather than 30–40 days after *B* maximum which is the case for normal SNe Ia. The light curve of SN 1998de deviates from that of SN 1991bg for about 20 days after the knee, but the two coincide at $t \approx 40$ days.

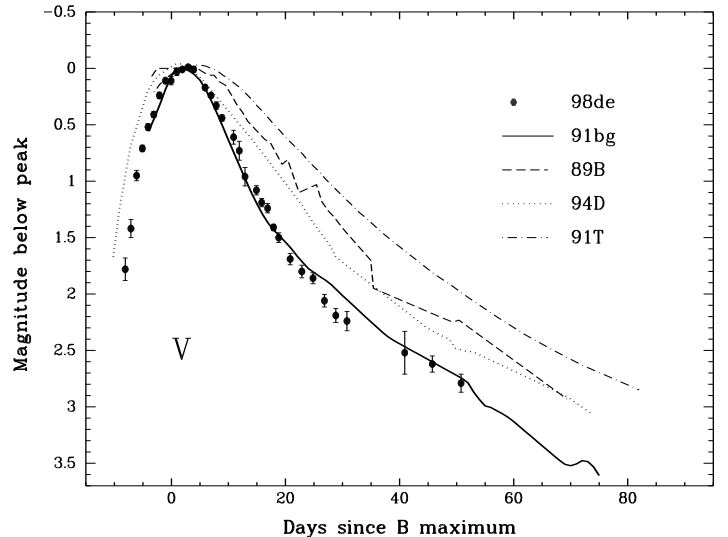


FIG 4. - Same as Fig. 3 but for the *V* light curve.

We present the *R*-band light curve in Figure 5 and note in SN 1998de the absence of the period of slower decline, the so-called “plateau,” which is characteristic of all normal SNe Ia at $t \approx 20$ to 30 days (Ford et al. 1993; Wells et al. 1994). Rather, SN 1998de fades monotonically in *R* at a rate of ~ 0.087 mag day⁻¹ between days 11 and 29, a bit slower than SN 1991bg (~ 0.092 mag day⁻¹, based on our analysis of F92 data). The slower decline of SN 1998de is also expressed by its smaller $\Delta m_{15}(R)$ value ($\Delta m_{15}(R) = 1.02 \pm 0.06$) when compared with that of SN 1991bg ($\Delta m_{15}(R) = 1.18$, based on our analysis of F92 data). There seems to be a region around the *R*-band maximum of SN 1998de, which is not smooth, but with the present data set we cannot assess the reality of this. Perhaps significantly, the apparent “wiggle” appears to be even more pronounced in the *I* band (Figure 6), though it may be due to an overall calibration problem with the data from that night.

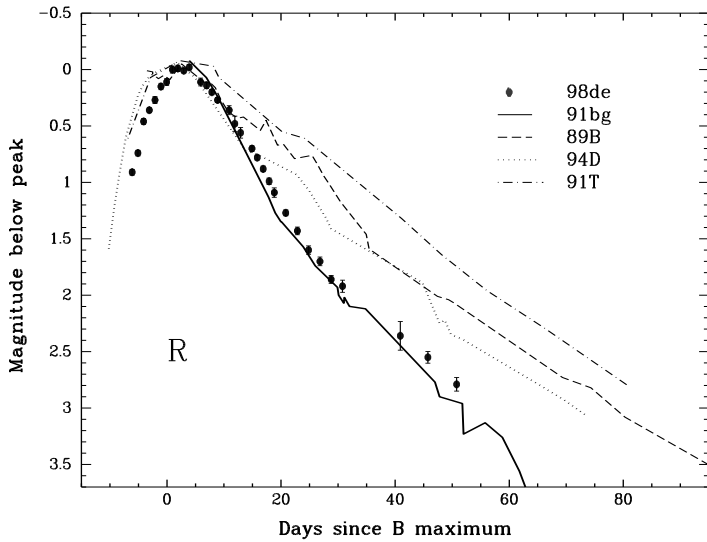


FIG. 5. - Same as in Fig. 3 but for the R light curve. The R light curve of SN 1991T comes from Ford et al. (1993). The R and I light curve of SN 1991bg come from F92.

After the initial peak in the I band 3–4 days past B maximum (Figure 6), there is a plateau that extends out to $t \approx 11$ days. However, the I band does not show the kind of second maximum whose prominence is usually expected of normal SNe Ia, again very similar to the I -band behavior of SN 1991bg (though the plateau in SN 1998de is more pronounced than that of SN 1991bg). The two other well-studied SN 1991bg-like events, SN 1992K (Hamuy et al. 1994) and SN1997cn (Turatto et al. 1998), were observed only well after maximum light, so that there is no range of overlap. More comparisons with new SN 1991bg-like objects are needed to see whether one maximum, two maxima, or a maximum plus plateau are typically present in these kinds of SNe Ia.

It is interesting to note that if the I -band light curve is treated as having one broad peak, then its maximum in I is reached 8 or 9 days later in SN 1991bg-like SNe Ia when compared to normal SNe Ia, falling between the two maxima exhibited by the latter. The derived $\Delta m_{15}(I)$ value is 0.69 ± 0.09 for SN 1998de and 0.88 for SN 1991bg (based on our analysis of F92 data).

We can also observe another trend, whose effect increases towards longer (redder) filter wavelengths: although SN 1998de seems to concur completely with SN 1991bg in the B filter at early times, the deviations become stronger in the other filters, with the post-maximum light curves declining more slowly than those of SN 1991bg. This trend is embodied in the smaller Δm_{15} in all passbands (except in B ; see Table 3) when compared with those of SN 1991bg.

In summary, then, the light curves of SN 1998de closely resemble those of SN 1991bg, and deviate notably from those of normal SNe Ia such as SN 1994D and overluminous ones like SN 1991T. However, there are significant differences between the light curves of SNe 1991bg and 1998de, especially at redder wavelengths, so we cannot simply regard SN 1998de as a mere twin of SN 1991bg. This conclusion, which is based on early- and intermediate-time photometry of SN 1998de, will be strengthened by the

intermediate- and late-time spectral analysis in §4.

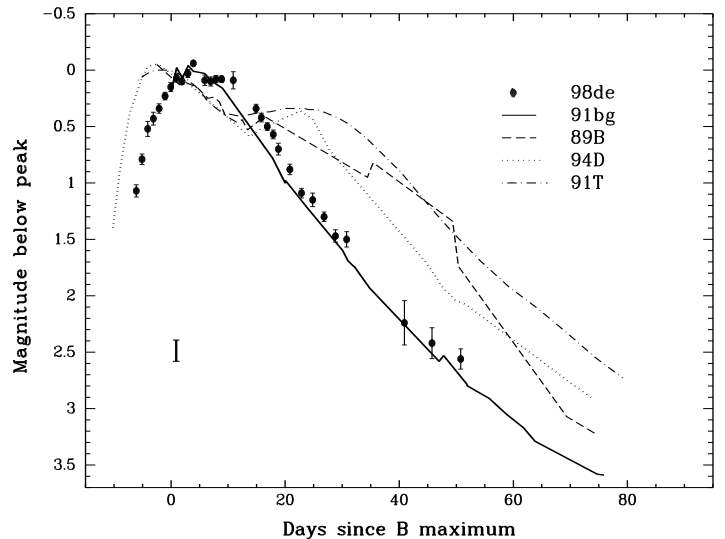


FIG. 6. - Same as Fig. 3 but for the I light curve.

2.3. Optical Color Curves

We denote any extinction-corrected quantity with a subscript zero, such as $(B-V)_0 = (B-V) - E(B-V)$; values which lack the subscript are not corrected for reddening. In Figures 7, 8, and 9, respectively we present the intrinsic optical color curves of SN 1998de, $(B-V)_0$, $(V-R)_0$, and $(V-I)_0$, together with color curves of several other SNe Ia (1991bg, 1989B, 1994D, and 1991T) for comparison. For SN 1998de, a Galactic reddening [giving rise to a color excess of $E(B-V) = 0.06$ mag] was derived using full-sky maps of dust infrared emission (Schlegel, Finkbeiner, & Davis 1998). In order to calculate the color excess for the I and R passbands we adopt the standard reddening law parameterization, $E(V-I)/E(B-V) = 1.60$ and $E(V-R)/E(B-V) = 0.78$ (Savage & Mathis 1979). We follow Wells et al. (1994) in correcting the data for SN 1989B with $E(B-V) = 0.37$ mag, and we assume reddenings $E(B-V)$ of 0.04 mag for SN1994D (Richmond et al. 1995), 0.13 mag for SN 1991T (Phillips et al. 1992), and 0 mag for SN 1991bg (F92).

We assume that there is negligible reddening due to the dust in the host galaxy of SN 1998de for the following reasons. SN 1998de is located $72''$ from the nucleus of the NGC 252, in the outskirts of a lenticular (S0) galaxy, where there is generally very little dust. Moreover, the spectra exhibit no conspicuous Na I D line at the redshift of the host galaxy. Unfortunately, we do not have enough $B-V$ points after $t = 32$ days in order to see whether the linear fit between intrinsic $B-V$ and time, which is described by Phillips et al. (1999) (and whose sample also includes SN 1991bg), is also valid for our case. The only measurement we have is $B-V$ at $t = 51$ days, which deviates from the Phillips et al. late-time color evolution by 0.39 mag; however, this point suffers from a large uncertainty. Nevertheless, we note that the late-time color evolution of $(V-R)_0$ and $(V-I)_0$, for which we have two more data points, seems to conform with the color evolution of normal SNe Ia, thus possibly indicating that there is very

little host galaxy extinction.

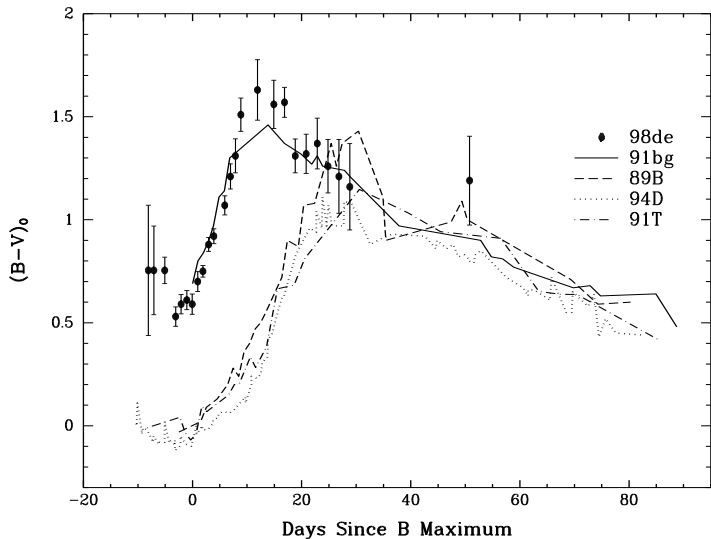


FIG. 7. - The $(B-V)_0$ color curve of SN 1998de, together with those of SN 1991bg (no reddening assumed), SN 1991T (dereddened by $E(B-V)=0.13$ mag), SN 1989B (dereddened by $E(B-V)=0.37$ mag), and SN 1994D (dereddened by $E(B-V)=0.04$ mag).

The prominent feature of the $(B-V)_0$ color evolution for both peculiar SNe (1991bg and 1998de) is their unusually red $(B-V)_0$ color at early epochs (Figure 7). At $t = -5$ days, SN 1998de has an observed $B-V$ color of 0.8 mag, which corresponds to an intrinsic color of $(B-V)_0=0.74$ mag for Galactic $E(B-V)=0.06$ mag. It first dips to the blue and then becomes progressively redder after $t = -3$ days, following a well-defined curve at a rate of ~ 0.04 mag day $^{-1}$, which concurs completely with that of SN 1991bg. At B maximum it has $(B-V)_0=0.59$ mag and SN 1991bg has $(B-V)_0=0.69$ mag, making SN 1998de about 0.6 mag redder than typical SNe Ia at this phase. Not only are the two peculiar SNe redder than normal SNe Ia, they also reach their reddest color (i.e., their maximum in a $B-V$ color curve) earlier than normal SNe Ia, at $t \approx 13$ days rather than at $t \approx 30$ days with $(B-V)_0^{max}=1.45$ mag for SN 1991bg and $(B-V)_0^{max}=1.63$ mag for SN 1998de. The subsequent decline of SN 1998de, its turning to the blue, conforms with that of SN 1991bg. The single late-time data point for SN 1998de is off by $\sim 0.3-0.4$ mag from all other SNe Ia. Since its uncertainty is very large and there are no other supporting data points, however, this observation is not conclusive.

The $(V-R)_0$ color curve of SN 1998de in Figure 8 shows a pattern of evolution which is again similar to that of SN 1991bg, but seems to be bluer at early phases ($t \lesssim 15$ days). The region between $t = -5$ and $t = 4$ days, for which there are no SN 1991bg data, seems to reveal a fairly stable color of $(V-R)_0 \approx 0.19$ mag. Between $t \approx 6$ and $t \approx 15$ days, the color of SN 1998de has a constant offset of ~ 0.12 mag to the blue, until it reaches its maximum at the same time as SN 1991bg, around 17 days after B maximum, with the same value of $(V-R)_0^{max} \approx 0.6$ mag. The distinctions between SN 1998de and the rest of the SNe Ia (except SN 1991bg) are significant enough to put the color

evolution of SN 1998de into a different category than that of normal SNe Ia. There may be a difference between the late-time color curves of SNe 1998de and 1991bg, but the data of both SNe are very noisy at that phase (see F92 for SN 1991bg).

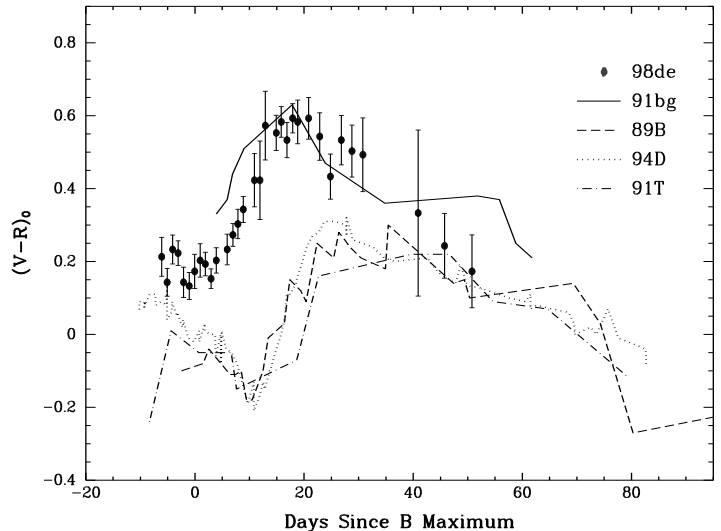


FIG. 8. - Same as in Fig. 7 but for the $(V-R)_0$ color curve..

Figure 9 shows the $(V-I)_0$ color evolution. Between $t = -5$ and $t = 4$ days, SN 1998de seems to display an almost constant color of $(V-I)_0 \approx 0.1$ mag. SN 1998de is 0.2–0.3 mag bluer than SN 1991bg at early times, but both objects reach their reddest color at about 17 days after B maximum. Whereas the color curve of SN 1998de is distinct from those of normal and overluminous SNe during early times, it may approximate them for $t \geq 40$ days.

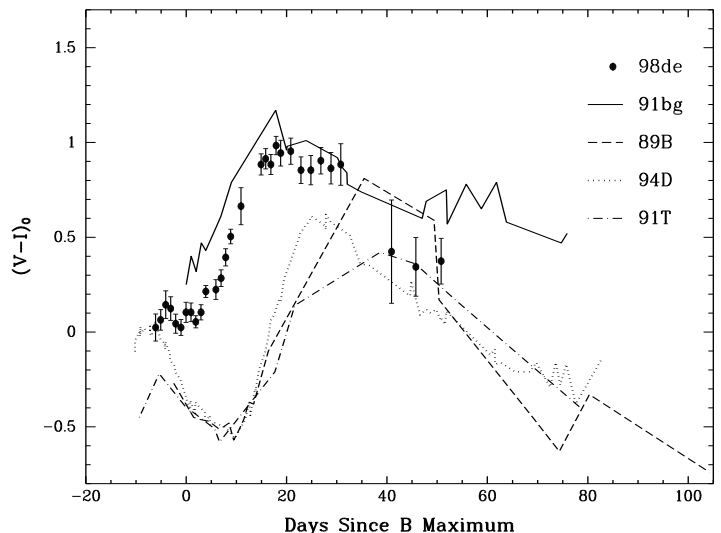


FIG. 9. - Same as in Fig. 7 but for the $(V-I)_0$ color curve.

Thus, the $(B-V)_0$, $(V-R)_0$, and $(V-I)_0$ color curves of SN 1998de generally have a similar pattern of evolution and are strikingly redder than those of normal and overluminous SNe Ia at early times ($t \lesssim 40$ days). Each color

TABLE 4
ABSOLUTE PEAK MAGNITUDES OF SEVERAL SNE IA

	B	V	R	I	source, note
1994D	-18.95 ± 0.18	-18.90 ± 0.16	-18.85 ± 0.15	-18.68 ± 0.14	1,a
1991bg	-16.54 ± 0.32	-17.28 ± 0.31	-17.58 ± 0.31	-17.68 ± 0.31	2,a
1998de	-16.97 ± 0.22	-17.67 ± 0.21	-17.84 ± 0.20	-17.81 ± 0.20	3,b

^aDistanced based on the surface brightness fluctuations (SBF) method.

^bMagnitudes for $H_o = 65 \text{ km s}^{-1} \text{ Mpc}^{-1}$. For $H_o = 75 \text{ km s}^{-1} \text{ Mpc}^{-1}$, add 0.31 mag to all magnitudes.

REFERENCES.—(1) Richmond et al. (1995); (2) Turatto et al. (1996); (3) this paper.

curve has a maximum with the time differing only slightly: 13 days after B maximum for the peak in $(B - V)_0$, and $t \approx 17$ days for $(V - R)_0$ and $(V - I)_0$.

3. ABSOLUTE MAGNITUDES

The light curves and color curves of SN 1998de suggest that it is subluminal, similar to SN 1991bg. In order to verify this, we need to find its absolute magnitude at maximum brightness and compare it with that of normal SNe Ia. Besides knowing the Galactic and extragalactic extinction, which was found in §2.3, we need to accurately determine the distance to the host galaxy NGC 252 (UGC 491, PGC 2819).

NGC 252 is listed as the brightest member of group 12 of the Lyon Group of Galaxies (LGC) Catalog (Garcia 1993) and also as a member of the Perseus supercluster (Vettolani & Baiesi Pillastrini 1987). It appears, however, that the values for the mean heliocentric radial velocities of the LGC 12 members given by Garcia (1993) are obsolete. The Lyon-Meudon Extragalactic Database⁵ (LEDA) developed by G. Paturel and last updated in October 1999, on which Garcia’s data are based, shows a systematic difference of $\sim 270 \text{ km s}^{-1}$ between its most current values and those of Garcia. Making use of LEDA, we obtain a mean heliocentric recession velocity of $cz = 4950 \text{ km s}^{-1}$ for NGC 252. This estimate is close to those obtained by several other groups using different methods (e.g., neutral hydrogen line-width measurements by Eder et al. 1991, optical measurements by Huchra et al. 1999; see also de Vaucouleurs et al. 1991), all of which are between 4949 and 5023 km s^{-1} .

Since there is no direct measurement (e.g., using Cepheids) of the distance to NGC 252, we must use the recession velocity and Hubble’s law for this purpose. However, this distance might not be accurate without corrections for gravitationally induced peculiar motions. Therefore, we adopt a corrected recession velocity of $v_{cor} = 5079 \text{ km s}^{-1}$ from LEDA, which accounts for our Local Group’s infall into the Virgo cluster. We can neglect the influence of the Virgo cluster on the host galaxy of SN 1998de, as indicated by Kraan-Korteweg (1986), and of peculiar motions induced by the Pisces-Perseus super-

cluster (of which NGC 252 is a member), as shown by Ichikawa & Fukugita (1992). Converting v_{cor} to a velocity in the cosmic microwave background (CMB) frame according to the prescription of de Vaucouleurs et al. (1991), we derive $v_{CMB} = 4754 \text{ km s}^{-1}$. Adopting a Hubble constant of $65 \pm 6 \text{ km s}^{-1} \text{ Mpc}^{-1}$ (Riess et al. 1998a; Jha et al. 1999), we find a distance of $73 \pm 7 \text{ Mpc}$ and a distance modulus of $\mu = (m - M) = 34.32 \pm 0.19 \text{ mag}$.

Using apparent peak magnitudes as listed in Table 3, together with our estimates of the extinction and distance, we derive the peak absolute magnitudes for SN 1998de in all filters (Table 4). The quoted uncertainties are the sums in quadrature of the uncertainties in peak magnitude, extinction, and distance. For comparison, we also list the absolute magnitudes of the subluminal SN 1991bg, as well as the normal SN Ia 1994D.

Riess et al. (1996, 1998a) describe an empirical method (the multicolor light curve shape; MLCS) to derive the absolute magnitude, distance, and total line-of-sight extinction of a Type Ia supernova. Applying the linear MLCS method to both light curves and color curves of SN 1998de, Riess (private communication, 2000) derives a value of the “luminosity correction” $\Delta = 1.42 \pm 0.15 \text{ mag}$ and $A_V = 0 \text{ mag}$. Given the uncertainties, this is indistinguishable from $\Delta = 1.44$ for SN 1991bg. The luminosity correction signifies the amount by which SN 1998de is dimmer at peak brightness than a normal SN Ia with $\langle M_V \rangle = -19.36 \text{ mag}$ (on the absolute Cepheid distance scale) — thus its absolute magnitude is $M_V = -17.94 \text{ mag}$. This value is 0.27 mag brighter than our more direct estimate, $M_V = -17.67 \text{ mag}$ (Table 4), but considering the uncertainties in both methods, this is not a very significant discrepancy. MLCS also suggests that there is no extinction, while we assumed $E(B - V) = 0.06 \text{ mag}$ of Galactic reddening. The MLCS method attempts to match the light curve of SN 1998de with that of the template, which is generated using a training set of SNe Ia. But since this training set consists primarily of normal SNe Ia and includes only one confirmed subluminal supernova (SN 1991bg) and a proposed one (SN 1986G; see, e.g., F92), MLCS might be less reliable at low luminosities. Thus, we hesitate to adopt

⁵www-obs.univ-lyon1.fr

the luminosity of SN 1998de derived by Riess.

We can clearly discern from Table 4 that SN 1998de is a subluminous supernova and that it has magnitudes similar to those of SN 1991bg [on the surface-brightness-fluctuations (SBF) distance scale⁶] in all four filters. These values are appreciably fainter and redder than the average, $M_B = -18.64(\pm 0.05) + 5 \log(H_o/85) = -19.22$ mag and $M_V = -18.59(\pm 0.06) + 5 \log(H_o/85) = -19.21$ mag for $H_o = 65 \text{ km s}^{-1} \text{ Mpc}^{-1}$ as found by Vaughan et al. (1995) for their *ridge-line* SNe Ia (i.e., SNe Ia that suffered little extinction, but were also not exceptionally luminous). SN 1998de is even more extreme when compared to the Riess et al. (1996) absolute magnitude template values ($M_V = -19.38$ and $M_B = -19.36$ mag) and the mean SN Ia magnitudes derived with the Cepheid distance calibration ($M_B = -19.65 \pm 0.13$ and $M_V = -19.60 \pm 0.11$ mag; see Saha et al. 1995).

4. SPECTROSCOPY

4.1. Observations and Reductions

Spectroscopic observations were conducted with the Lick 3-m Shane telescope using the Kast CCD spectrograph (Miller & Stone 1993) on the three dates listed in Table 5. The air mass was in all cases close to 1.0, and a slit width of $2''$ was used.

TABLE 5
Journal of Spectroscopic Observations^a

UT Date	J.D.—	Phase
DD/MM/YY	2, 451, 000.0	(days)
31/08/98	56.8	+31
20/09/98	76.8	+51
15/10/98	101.7	+76

^a Lick 3-m reflector, 3,400–10,000 Å.

All optical spectra were reduced and calibrated employing standard techniques. To remove near-infrared fringing in the CCD, flatfield exposures were taken at the position of the supernova, as were He-H-Cd-Ne-Ar lamp exposures for wavelength calibration. The spectra were corrected for the continuum atmospheric extinction using mean extinction curves, and their telluric lines were removed following a procedure similar to that of Wade & Horne (1988) and Bessell (1999). The final flux calibrations were derived from observations of one or more spectrophotometric standard stars (Oke & Gunn 1983). All spectra shown in this paper have been corrected for reddening (as in §2.3) and for their redshift.

The spectral evolution of SN 1998de is illustrated in Figure 10. There was poor signal below 4000 Å and considerable fringing above 8000 Å, especially at late times. The sharp and narrow “absorption lines” in the $t = 76$ d spectrum are most surely noise spikes. We refrained from averaging or smoothing those features in order to give an authentic impression of the quality of the data.

As mentioned in §2.1, the spectrum reported by Garnavich et al. (1998) and taken ~ 6 days before B maximum already shows the Ti II absorption feature and a very strong Si II feature at 5800 Å, suggesting SN 1998de to be a SN 1991bg-type Ia event. Unfortunately, we have no spectra of our own around maximum light, for which we

could have directly used the spectral sequencing method described by Nugent et al. (1995) to apply their derived correlations with the absolute B magnitude. Our first spectrum was obtained 31 days after B maximum and resembles that of the peculiar SN Ia 1991bg. It exhibits the broad trough at 4100–4500 Å identified as Ti II (F92; T96; M97) and shows signs of an early onset of the nebular phase. On the other hand, apparent evidence for abundance or excitation anomalies is present when compared with SN 1991bg.

In general, the evolution of the supernova can be separated into two phases: the photospheric phase, which lasts from the time of explosion until around 40 days after B maximum for normal SNe Ia, and the subsequent nebular phase. During the photospheric phase, the supernova and its ejecta are optically thick, so the spectrum forms at and above the photosphere and reflects the abundances of the elements constituting the outermost layers. Here the radiative transfer effects are of paramount importance, since the observable spectrum is produced by a series of photon emissions, absorptions, and scatterings resulting in overall line blending. Unambiguously identifiable P-Cygni profiles formed by resonant scattering above the photosphere are rare. We expect to see more traces of intermediate-mass elements from oxygen to carbon in the spectra during the photospheric phase than during the nebular phase, since the outer high-velocity layers are assumed to consist of products situated in the middle of the nuclear burning chain with iron-peak elements as the ending points (e.g., Branch et al. 1983; Kirshner et al. 1993). At this stage absorption lines are more easily identifiable than emission lines. The transition period, when the photosphere recedes into the center (i.e., when the ejected material is becoming transparent), is marked by the rising prominence of emission lines. During the subsequent nebular phase, the spectrum formation happens primarily in the deep layers of the ejected matter consisting of iron-group isotopes (Axelrod 1980; Ruiz-Lapuente et al. 1995).

In the following, we adopt the line identifications for SNe Ia of Jeffery et al. (1992), Kirshner et al. (1993), and also those of F92, L93, T96, and M97 for SN 1991bg-type events. Since the L93 absorption identifications refer only to the phase of B maximum and are not applicable at later epochs, we employ them with caution. We note that our line identifications for SN 1998de are not definitive since we have not conducted spectral synthesis calculations. The identification of emission lines, especially, on the basis of wavelength coincidences might be a precarious undertaking; due to the presence of a complex blend of P-Cygni profiles on an underlying spectrum that varies rapidly with wavelength, the wavelengths of the emission peaks may be affected. We adopt the convention that wavelengths given in Å are measured wavelengths in the restframe of the galaxy, whereas those preceded by a λ are laboratory wavelengths.

To illustrate the similarities and differences among SN 1998de, its close relative SN 1991bg, and the normal SN Ia 1994D, we plot the three epochs separately in Figures 11, 12, and 13. Although SN 1998de shares several of SN 1991bg’s unusual features in the wavelength range corresponding to the B band, it also exhibits notable dis-

⁶Note that the SBF method yields a Hubble constant of $\sim 75 \text{ km s}^{-1} \text{ Mpc}^{-1}$ (e.g., Tonry et al. 2000)

parities in the wavelength ranges of the V , R , and I bands. This is consistent with the trend seen in the light curves of SN 1998de, where the deviation from SN 1991bg increases with increasing band wavelengths. Thus, a good match in one passband (here the B band, perhaps the most frequently observed one) does not necessarily guarantee the same degree of similarity in the other passbands. This has ramifications for further studies of peculiar SNe Ia, calling for a broad passband coverage in both photometric and spectroscopic observations.

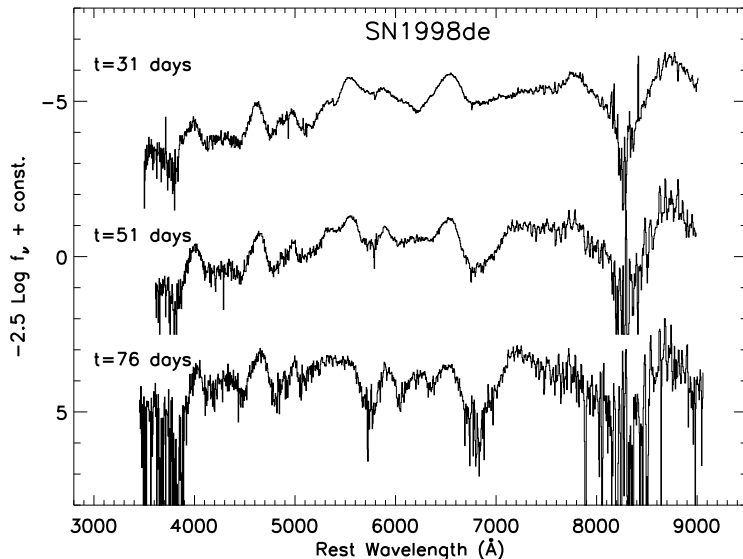


Fig. 10. - Montage of spectra of SN 1998de. The phases marked are relative to the date of B maximum. To improve clarity, the spectra have been shifted vertically by arbitrary amounts. The effective units on the ordinate are magnitudes ($-2.5 \log f_\nu + \text{const.}$). Unless otherwise noted, all spectra in this paper are shown in the rest system of the host galaxy and corrections for reddening have been made. Note that the well-defined notch at the 5794 Å (5891 Å in the observed frame) is most probably due to improper subtraction of a night-sky emission line at an observed wavelength of 5893 Å.

4.2. The Spectrum at 31 Days after B Maximum

In the $t = 31$ d spectrum (Figure 11), Ca H&K is seen in both absorption and emission as a classical P-Cygni profile, as expected for SNe Ia. However, whereas the emission component (at 3990 Å) stays the same, the absorption part (at 3790 Å) deepens as the object ages (Figure 10, although it is hard to discern its exact strength due to noise and the absence of any other emission features at shorter wavelengths), similar to the trend observed with SN 1991bg, where it grew even deeper. The broad absorption trough between 4120 and 4460 Å, one of the most conspicuous and intriguing peculiarities of all very subluminal SNe Ia, such as SN 1991bg, has been identified with Fe III by L93 by matching wavelengths, while F92, Ruiz-Lapuente et al. (1993), and M97 attribute it to a blend of Ti II lines using spectral synthesis analysis. F92 and M97 suggest that Mg II $\lambda 4481$ might also contribute to the absorption. Since the evidence for Ti II through the technique of spectral synthesis is more compelling, we

adopt this particular interpretation. This trough contrasts sharply with the expected blend of Si, Mg, and Fe lines observed at comparable epochs in typical SNe Ia (e.g., Kirshner et al. 1993). Note that the trough in SN 1998de might be somewhat broader (by ~ 100 Å) than the one in the SN 1991bg spectrum.

The wavelength range between 3800 Å and 5540 Å provides an impressive match to that of SN 1991bg. The emission line at about 5540 Å has been attributed to [O I] $\lambda 5577$ for SN 1991bg by F92 [see L93 for an alternative identification], indicating the early start of the nebular phase. If we apply this identification also to SN 1998de, a significant fraction of the unburnt oxygen is visible in dense states outside the bulk of the ejecta, as suggested by M97 for SN 1991bg. L93 reject this interpretation, since the strength of the line and the absence of the [O I] doublet at 6300 Å would imply very high densities ($n \approx 10^{11}$ oxygen atoms cm^{-3}) and low temperatures ($T_e \leq 2000$ K) for reasonable electron density ($n_e/n_{\text{O II}} = 1$) and ionization ($n_{\text{O II}}/n_{\text{O I}} = 10^{-2}$; L93). However, M97 present compelling and intriguing evidence with the use of Monte Carlo simulations that SN 1991bg shows an indication of a high oxygen abundance due to incomplete burning and low temperatures. Their calculations may also explain the unusual strength of the Ti II lines and the red color of SN 1991bg.

Broad emission features, which are stronger in both SN 1991bg and SN 1998de than in SN 1994D and which are commonly observed in normal SNe Ia at later epochs ($t \gtrsim 40$ days), are the emission components of the Ca H&K feature and of the Ca II near-infrared triplet at 8700 Å, implying an early onset of the nebular phase.

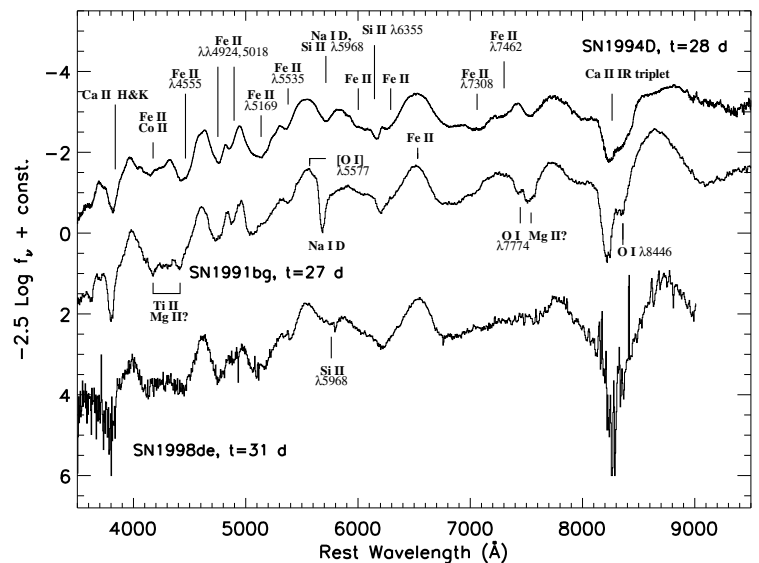


FIG 11. - The spectrum of SN 1998de about 4 weeks past maximum brightness, shown with comparable-phase spectra of SN 1991bg (no reddening assumed) and of the normal SN Ia 1994D (dereddened by $E(B - V) = 0.04$ mag). See text for sources of line identifications.

One of the most unusual characteristics displayed by the intermediate and late-time spectra of SN 1991bg is a very strong and relatively narrow absorption line mea-

sured near 5700 Å, which increases in strength over time. As T96 show, this line, which is almost invisible in the maximum-light spectrum, persists for over 5 months with the line profile remaining nearly constant in time (FWHM ≈ 2500 km s⁻¹). If we identify it with Na I D (F92; see Fig.7 of M97 for the reproduced Na I D line in a modeled spectrum), which indeed forms a broad absorption line in normal SNe Ia at this epoch, we obtain an expansion velocity of $v_{\text{Na I D}} = 9400$ km s⁻¹ for the absorbing layers. This is larger than the corresponding expansion velocity derived on the basis of the Si II $\lambda 6355$ shift for the same epoch ($v_{\text{Si II}} = 7000$ km s⁻¹). Both the narrow width and the high expansion velocity indicate that the element responsible for the 5700 Å feature is situated in a relatively thin outer layer (since the velocity of a shell is proportional to its radius at this phase). This could be evidence for abundance stratification in the ejecta of SN 1991bg as pointed out by T96. An alternative interpretation is given by L93, who propose that the 5700 Å feature is due to a blend of Si II lines, but since it is very narrow, we hesitate to adopt this identification (although Si II might be present, but contaminated by the very strong Na I D).

Remarkably, the 5700 Å feature is not visible in any of the SN 1998de spectra, whereas other SN 1991bg-type objects like SN 1997cn (Turatto et al. 1998) and SN 1992K (Hamuy et al. 1994) display it. SN 1998de thus adds to the “mystery” of this conspicuous feature. It is interesting that the first major mismatch between SN 1998de and SN 1991bg occurs in the passband corresponding to the *V* band. It is tempting to correlate the photometric mismatch found in the *V* filter for $t = 31$ days (SN 1998de being ~ 0.2 mag dimmer than SN 1991bg) with the 5700 Å feature and other, minor lines.

In SN 1998de, as in SN 1991bg, the primary characteristic feature of SNe Ia, Si II $\lambda 6355$, seems to be contaminated by another absorption line. Unlike the case in SN 1991bg, however, both wings appear to be broadened owing to the presence of other elements. Instead of a narrow and well-defined core as found in normal SNe such as SN 1994D, we see a V-shaped feature that fades as the supernova ages. Garnavich et al. (1998) measure at $t = -6$ days the minimum of Si II $\lambda 6355$ at 6185 Å and thus infer a photospheric expansion velocity of 13,300 km s⁻¹ for SN 1998de, after correcting for the host galaxy’s redshift. This is consistent with expansion velocities for normal SNe Ia which range between 11,000 and 13,000 km s⁻¹ at maximum brightness (Branch et al. 1988; Barbon et al. 1990), and possibly with SN 1991bg, which showed a velocity of 9900 km s⁻¹ at maximum light (F92). Applying the same technique we find an expansion velocity of 7080 km s⁻¹ for $t = 31$ days, which is in excellent agreement with a velocity of ~ 7000 km s⁻¹ for SN 1991bg at $t = 27$ days and considerably smaller than the photospheric expansion velocity of SN 1994D ($v = 8970$ km s⁻¹) at the same epoch⁷. These results are very interesting: whereas SN 1991bg showed a consistently lower expansion velocity than normal SNe Ia, which led to the theoretical insights that the mass of the ejecta might be small for consistency with an early onset of the nebular phase and that complete burning was confined to the innermost regions (T96; M97), SN 1998de might not

show such a clear trend. Again, early-time spectra would have been more useful for monitoring the development of the expansion velocity.

Note the broad emission near 6520 Å, which usually begins to develop around $t = 2$ weeks for normal SNe Ia and which is clearly visible at $t \approx 4$ weeks in the spectra of SNe 1994D, 1991bg, and SN 1998de. It remains present thereafter with some changes in shape and can be identified with Fe II and later [Fe II] (L93; Filippenko 1997), and not with H α as one might erroneously infer.

A peculiarity which distinguishes SN 1998de from both SN 1991bg-like objects and normal SNe Ia is the nearly featureless region from 6800 Å to 7600 Å which lies in a wavelength range corresponding to the *I* passband. The prominent absorption component of the O I $\lambda 7774$ P-Cygni feature and its contamination by Mg II $\lambda 7877-7896$ in the red wing as seen in SN 1991bg (F92; M97; T96) and its twins (SNe 1997cn, 1992K) is not present, whereas the hump near 7760 Å is probably due to the emission component of O I $\lambda 7774$ (but at a slightly longer wavelength when compared to SN 1991bg; L93; F92; M97). The spectrum of SN 1998de may show a small indentation at the expected position of Mg II, but the quality of the data is too poor for a definite conclusion. M97 claim that the observed behavior of the O I $\lambda 7774$ absorption in SN 1991bg, which does not evolve redward (i.e., to lower velocities) during the first two weeks after *V* maximum, is indicative of an outer oxygen shell containing unburned material from the progenitor, for which the observed [O I] $\lambda 5577$ emission was the first clue. The absence of the O I $\lambda 7774$ absorption line in SN 1998de could be due to possible contamination by a blend of broad emission lines, but no likely candidates are known. A more feasible explanation could be that there is not as much [O I] present in SN 1998de as in SN 1991bg. If so, perhaps SN 1998de does not have as much unburnt oxygen left as did SN 1991bg.

As in other SN Ia spectra, the obvious P-Cygni profile of the Ca II near-infrared triplet is visible between 8000 Å and 8700 Å, although both absorption and emission are much stronger than usual, similar to the appearance of SN 1991bg. Early-time spectra would be more conclusive for displaying the effects of color evolution — indeed, we would expect those spectra to be redder than in normal SNe Ia. The consistently red color of SN 1991bg was interpreted by M97 as an indication for a lower photospheric temperature, as would be expected with the presence of only incomplete nuclear burning.

4.3. The Spectra at 51 and 76 Days after *B* Maximum

Figure 12 displays the spectra of SNe 1998de, 1991bg, and 1994D at about the same epoch of $t \approx 7$ weeks, while Figure 13 shows the spectra of the same SNe at $t \approx 12$ weeks. Our initial conclusion — that differences between SN 1998de and SN 1991bg increase with increasing wavelength — is confirmed. Besides the further emergence of emission lines, the following major changes have occurred in SN 1998de, and are clearly visible in Figure 13: (1) the [O I] $\lambda 5577$ and the O I $\lambda 7774$ emission features have weakened and become broader; (2) pronounced emission has appeared at 5900 Å whose position coincides with the

⁷Since the Si II $\lambda 6355$ line is not visible in later spectra, we cannot use it to obtain the expansion velocity, but by then the nebular phase has completely emerged and the photospheric model is no longer applicable.

[Co III] emission in SN 1991bg (L93; T96; M97); (3) a deep and broad absorption trough is present at $\sim 6800 \text{ \AA}$ adjacent to an emerging broad emission feature at $\sim 7200 \text{ \AA}$; and (4) Si II $\lambda 6355$ has disappeared whereas Si II $\lambda 5968$ seems to have gained strength and may be contaminated in its blue wing.

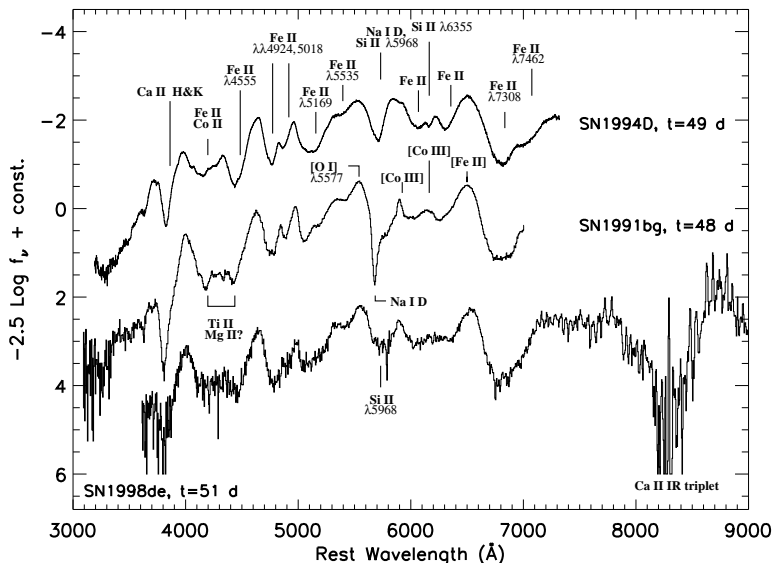


FIG 12. - Same as in Fig. 11 for SNe Ia about 7 weeks past maximum.

Most of the emission lines at this nebular stage are identified with forbidden lines of Fe and Co, the decay products of ^{56}Ni , while the Ca II emission is still strong in the spectra of both SN 1998de and SN 1991bg (Figure 13). The oxygen line deterioration can be explained by the fact that the photosphere is receding into the central parts of the ejecta, where the higher-mass elements have been produced. The drifting of emission lines to the red, most notably the [Fe III] feature at 4615 \AA , illustrates the decrease in the expansion velocity as we look deeper into the ejecta. The broad absorption at 6800 \AA is most probably due to Fe II, whose signature is visible in SN 1991bg as well as in SN 1994D (and generally in SNe Ia). The adjacent emission at 7200 \AA , which is only visible at $t = 76$ days, could be tentatively identified as a blend of [Ca II] $\lambda\lambda 7291, 7324$ (F92; Ruiz-Lapuente et al. 1993) or a blend of [Fe II] (L93). Note that the corresponding feature in SN 1991bg is observed at a slightly longer wavelength (7250 \AA) and that it dominates the spectrum of SN 1991bg, whereas it is very broad and not as distinct in the spectrum of SN 1998de (also the red shoulder seems to be contaminated), and is absent in the case of SN 1994D.

Since the Si II $\lambda 5968$ absorption is not contaminated by a Na I D line, it is easily visible as a distinct feature at nearly the same position as in the $t = 31$ d spectrum, only deeper. Because this Si II feature deepens between the two last epochs and is accompanied by a receding photosphere which reveals the deeper layers, we could have evidence that nuclear burning was incomplete in these layers.

The dominant and narrow [Co III] emission feature of SN 1991bg visible at 5908 \AA has been regarded by M97 as

an indication of a centrally peaked distribution of ^{56}Ni and as the result of complete incineration of matter in the central part of the ejecta, assuming that the emissivity is proportional to the Co abundance and to the local gamma-ray deposition rate in the Co-rich material. Combining this with their observation of oxygen during the photospheric phase, M97 suggest that complete burning did not take place everywhere, and that the outer layers underwent incomplete burning in contrast to the inner part. For SN 1998de, the corresponding [Co III] emission is observed at nearly the same position of around 5900 \AA in both the $t = 51$ d and the $t = 76$ d spectra; however, it is not as narrow as in SN 1991bg. This might indicate that complete incineration extended to a larger radius in SN 1998de than it did in the case of SN 1991bg. [Co III] $\lambda\lambda 6129, 6197$ emission is also found at around 6210 \AA in the $t = 76$ d spectrum, matching the features at 6144 \AA and 6204 \AA in SN 1991bg (T96). Furthermore, we see the afore-mentioned emission of [Fe II] (L93; see T96 for alternative identification) at around 6520 \AA in the spectrum of SN 1998de, a feature which is found in all three SNe (1994D, 1991bg, 1998de) and which was already visible in their intermediate-phase spectra (see Figure 11).

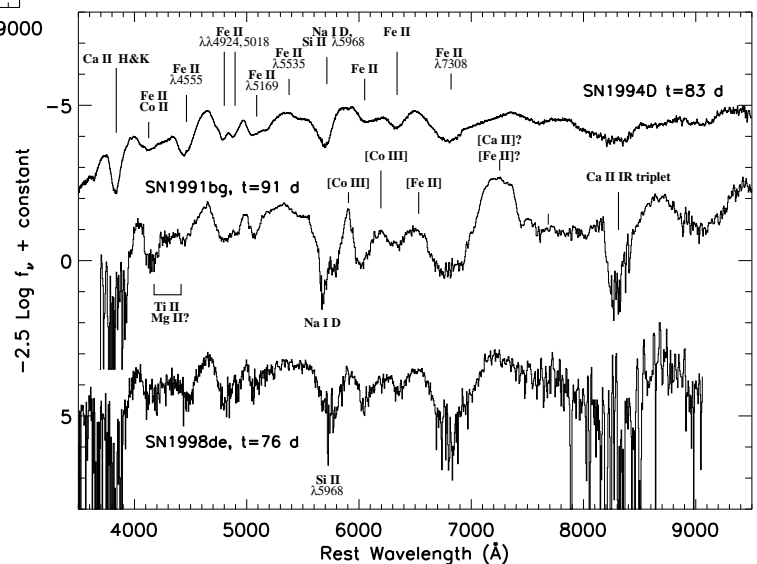


FIG 13. - Same as in Fig. 11 for SNe Ia about 12 weeks past maximum.

The Ti II trough between 4100 \AA and 4500 \AA , a primary characteristic of SN1991bg-type objects, is still distinctly visible at these late times. Thus, this feature can be used as a powerful tool for distinguishing between peculiar and normal SNe Ia at all epochs, even for SNe at large redshifts (whose restframe visible and red spectral regions are shifted into the range where the infrared fringing of CCDs affects the data). The strong presence of Ti II can be explained either in terms of abundance anomalies or by excitation differences. Both F92 and M97 favor the interpretation that the red color and hence low excitation temperature is largely responsible for producing the observed strong Ti II lines in local thermodynamic equilibrium (LTE; see, e.g., Fig. 1 of Branch 1987) and, simul-

taneously, the higher-excitation lines of the other ions like Ca II.

5. DISCUSSION

In SNe Ia, the energy of the initial explosion gained through thermonuclear fusion is used up by the adiabatic expansion of the ejecta (e.g., Leibundgut & Pinto 1992), whereas the light curve is powered by the decay of radioactive ^{56}Ni and ^{56}Co . It is also believed that there is a direct link between the mass of the ^{56}Ni produced during the explosion and the peak bolometric luminosity (see, e.g., Arnett, Branch, & Wheeler 1985; Höflich et al. 1996). Assuming that the observed low *optical* luminosity of SN 1998de is indicative of its bolometric luminosity, we can conclude that the mass of the synthesized nickel was smaller than in normal SNe Ia. M97 derive a value of $\sim 0.07 M_{\odot}$ of synthesized ^{56}Ni for SN 1991bg, which agrees well with the original estimate of Ruiz-Lapuente et al. (1993) of 0.05 to 0.1 M_{\odot} and which is a factor of 4 to 8 smaller than in normal SNe Ia. We could expect that similar amounts of nickel have been produced in both SN 1991bg and SN 1998de, as both SNe exhibit similar absolute magnitudes in all filters. However, spectral synthesis calculations and bolometric light curves are necessary for obtaining a definitive value for the nickel mass.

On the other hand, there are a number of indications, which suggest that SN 1998de might have experienced a slightly more powerful explosion than SN 1991bg did. Among these are the slower decline of the light curves in the *V*, *R*, and *I* bands and the offset of the color curves toward the blue. The fact that SN 1998de appears to show the same luminosities when compared with SN 1991bg (on a distance scale using $H_0 = 75 \text{ km s}^{-1} \text{ Mpc}^{-1}$) is only mildly inconsistent with the other pieces of evidence.

The models which have been proposed to explain the physics of SNe Ia in the last 30 years can be divided into two main categories: those that describe different explosion mechanisms with the same progenitor system, and those that propose different systems as the reason for the heterogeneity of SNe Ia and in particular as production sites of subluminescent SNe Ia. Despite the partial success of various models (see reviews by, e.g., Woosley & Weaver 1986; Wheeler & Harkness 1990; Branch et al. 1995; Livio 1999; Hillebrandt & Niemeyer 2000), no general consensus about the exact character of the explosion mechanism and the evolutionary track that leads to the SN Ia event has yet been reached.

The classical explosion models assume that a SN Ia is the thermonuclear disruption of a carbon-oxygen white dwarf in a close binary system that reaches the Chandrasekhar limit of $1.4 M_{\odot}$ by accreting mass from its companion star. They describe how the burning front or flame propagates through the white dwarf and comprise three general classes: (1) deflagration, (2) detonation, and (3) delayed detonation. The detonation model (see, e.g., Arnett 1969) postulates that the speed of the burning front is supersonic, and that the density and pressure increase behind the burning front. The deflagration model (see, e.g., Nomoto, Thielemann, & Yokoi 1984), on the other hand, suggests that the explosion behaves like a flame, where the burning front advances more slowly than the local sound speed and where the density and pressure decrease leading to a turbulent convective propagation. The

delayed detonation model is a variation on the first two, since it suggests that the flame starts as a deflagration and accelerates into a detonation later (see, e.g., Khokhlov, Müller, & Höflich 1993). The problem with a pure detonation model is that it predicts only iron-peak elements (and helium), whereas observations reveal the presence of intermediate-mass elements like calcium, sulfur, and silicon. The deflagration model seems to concur better with observational data, although some form of detonation at the late stages might be involved. According to Nomoto, Thielemann, & Yokoi (1984), the deflagration wave reaches the outer layers of the white dwarf where the temperature is too low to complete silicon burning, and thus produces the intermediate-mass elements.

Höflich, Khokhlov, & Wheeler (1995) used the pulsating class of delayed detonation models to establish the principle that Chandrasekhar mass C-O white dwarf models give a common explosion mechanism accounting for both normal *and* subluminescent SNe Ia, with SN 1991bg as their example for the latter group. However, as T96 correctly point out, their model requires a large reddening for SN 1991bg [$E(B - V) = 0.30 \text{ mag}$] in order to harmonize the theoretical luminosity with the observed value, while observations indicate a much smaller value close to zero (F92; T96; L93). Also, the decline rates of their SN 1991bg models are similar to those of their normal SN Ia models, while SN 1991bg is observed to be much faster.

As mentioned by F92 and others, an alternative scenario for subluminescent SNe Ia might involve ejecta with mass appreciably *smaller* than the Chandrasekhar limit that would account for several of the peculiar features of SN 1998de. The trapping of gamma rays produced by the decay of ^{56}Ni and ^{56}Co would be less effective due to the low column depth of the ejecta, thus leading to the rapid decline in the observed *BVRI* light curves after maximum light and possibly to the low optical luminosity. Also, low-mass ejecta expanding at only a slightly slower velocity than in normal SNe Ia would allow the photosphere to recede more quickly than usual, revealing the deeper layers and giving rise to the early emergence of the nebular spectrum.

The decline in photospheric expansion velocity from $\sim 13,000 \text{ km s}^{-1}$ at $t = -6$ days (Garnavich et al. 1998) to 7080 km s^{-1} at $t = 31$ days might be consistent with that of SN 1991bg, which showed an expansion velocity of $\sim 7000 \text{ km s}^{-1}$ at $t = 27$ days. Unfortunately, there are no other data points available for SN 1998de, especially since photospheric velocities are not defined during the nebular phase (i.e., for our last two spectra), and no premaximum spectra are available for SN 1991bg.

The consistently small velocity observed in SN 1991bg was interpreted by T96 as a possible indication that complete nuclear burning was confined to the innermost regions. Other phenomena which are thought to support this conclusion are the high abundance of oxygen (suggested by the [O I] $\lambda 5577$ and O I $\lambda 7774$ lines) left over from the progenitor (M97; T96), and the narrow [Co III] emission at 5908 \AA . Using the presence and strength of those features as observed in SN 1998de, we might infer that the inner region of complete burning was somewhat larger in SN 1998de than in SN 1991bg; indicators include the weaker appearance of O I $\lambda 7774$ and the somewhat

broader [Co III] emission at 5900 Å in SN 1998de. Furthermore, the hypothesis that SN 1998de might have experienced a slightly more powerful explosion than SN 1991bg did is consistent with this model. The red color of both SNe 1998de and 1991bg seems to implicate a low excitation temperature which gives rise to the Ti II trough found at the blue end of the spectrum without requiring an overabundance of titanium.

Here, we briefly review some of the scenarios proposed to explain the ejection of a sub-Chandrasekhar envelope. Livne (1990), Woosley & Weaver (1994), and Höflich & Khokhlov (1996) suggest that the *progenitor* itself has a mass below the Chandrasekhar limit. According to their models, a sub-Chandrasekhar-mass C-O white dwarf detonates due to the ignition of an outer He shell accumulated on top of it. Their predictions include a lower luminosity, a lower production rate of nickel, and an overabundance of titanium. In addition, the observed light curves can be adequately reproduced with this model. The absence of unburned He in the spectra might be explained by the low excitation temperatures present. On the other hand, they predict bluer colors at maximum brightness, while SNe 1991bg and 1998de are very red at that phase, as well as an outer Ni shell, which has not been observed in any of the subluminescent SNe Ia. Moreover, they do not account for the outer oxygen shell.

Another possibility might be a double-degenerate system of intermediate-mass C-O white dwarfs that merge, giving rise to the disruption of the less massive star, followed by the formation of a thick, hot accretion disk around the more massive companion and the subsequent explosion of the remaining white dwarf when it reaches the Chandrasekhar limit (e.g., Iben & Tutukov 1984; Webbink 1984). As a consequence only a small mass of ^{56}Ni would be produced, and there would be a mixture of burnt and unburnt material as observed in SN 1991bg and SN 1998de. However, the outcome of such a coalescence is still not completely understood; there are strong indications that it may rather lead to an accretion-induced collapse forming a neutron star than to a SN event (see, e.g., Saio & Nomoto 1985, 1998; Woosley & Weaver 1986; Mochkovitch & Livio 1990, Mochkovitch et al. 1997).

Unfortunately, none of the proposed models unambiguously emerges as the preferred candidate for explaining subluminescent SNe Ia, since each of the models appears beset by some problems as discussed above. Detailed studies of more subluminescent SNe are needed to provide additional constraints for the models. Indeed, the ongoing efforts of LOSS to conduct photometric follow-up observations of recently discovered subluminescent SNe Ia promise to contribute significantly; the results will be discussed by Li et al. (2001).

6. CONCLUSIONS

We have presented a set of photometric and spectroscopic observations of the recent SN 1998de, which reveal it to be an intrinsically faint SN Ia, similar to, but not identical with SN 1991bg. Similarities include (1) the intrinsically low luminosity (2) the remarkably red colors near maximum; (3) the narrow peak in all bands; (4) the rapid and monotonic decline of the light curves, includ-

ing in the *I* band; (5) the strong Ti II absorption lines throughout all observed epochs; (6) the early transition to a nebular spectrum; and (7) the strong [Ca II] emission lines at late times. The very good coverage of the *BVRI* light curves together with their high quality and early start make SN 1998de a defining template for subluminescent SNe Ia.

Whereas the *B* passband provides the best early-time match between SN 1991bg and SN 1998de, the deviations in both light curves and spectra between the two SNe Ia seem to increase toward longer (redder) wavelengths. Features of SN 1998de that distinguish it from SN 1991bg include (1) a plateau phase (or a possible second maximum) in the *I* band, very shortly after the first maximum; (2) a slower decline of the light curves in the *V*, *R*, and *I* bands; (3) slightly bluer colors at intermediate phases; (4) the absence of the conspicuous Na I D absorption found at 5700 Å in the spectra of SN 1991bg; and (5) the evolution of a region (6800–7600 Å) in the spectra of SN 1998de from featureless to feature-rich. Our comparison of SN 1998de and SN 1991bg may imply that subluminescent SNe Ia are not fully described as a one-parameter [$\Delta m_{15}(B)$] family. The somewhat slower decline rates and bluer colors combined with the evidence that the region of complete burning was larger in SN 1998de than in SN 1991bg, suggest that SN 1998de might have experienced a slightly more powerful explosion than SN 1991bg did.

The observed peculiarities of SN 1998de (and of SN 1991bg) might be explained in terms of ejecta with a mass smaller than that found in normal SNe Ia. However, at this time Chandrasekhar-mass models seem to provide an equally acceptable explanation.

Our analysis strengthens the conclusion that SN 1991bg was not a unique event, as already proposed by studies of several other intrinsically dim SNe Ia. Further conclusions to be drawn — besides the insights into the intrinsic workings of SNe Ia — concern the implications of our observations for the standard-candle assumption of SNe Ia and for their usage as cosmological distance indicators. We propose that intrinsically subluminescent SNe Ia should be identified in samples of SNe Ia used for cosmological purposes, with the Ti II trough at the blue end of the spectrum and the absence of a clear secondary maximum in the *I* band as possible criteria. It is advisable that the standard calibration methods be applied with caution on such objects; for example, the “snapshot” method of deriving distances of SNe Ia (Riess et al. 1998b) currently assumes that the objects are normal.

The work of A. V. F.’s group at U. C. Berkeley is supported by the National Science Foundation grants AST-9417213 and AST-9987438. KAIT was made possible by generous donations from Sun Microsystems, Inc. (Academic Equipment Grant Program), Photometrics Ltd., the Hewlett-Packard Company, AutoScope Corporation, the National Science Foundation, the University of California, Lick Observatory, and the Sylvia and Jim Katzman Foundation. We thank Adam G. Riess for many useful discussions.

REFERENCES

- Arnett, W. D. 1969, *Ap&SS*, 5, 180
- Arnett, W. D., Branch, D., & Wheeler, J. C. 1985, *Nature*, 314, 337
- Axelrod, T. S. 1980, in *Type Ia Supernovae*, ed. J. C. Wheeler (Austin: University of Texas), p.80
- Barbon, R., Benetti, S., Cappellaro, E., Rosino, L., & Turatto, M. 1990, *A&A*, 237, 79
- Bessell, M. S. 1999, *PASP*, 765, 1426
- Branch, D. 1987, *ApJ*, 320, L121
- . 1998, *ARA&A*, 36, 17
- Branch, D., Lacy, C. H., McCall, M. L., Sutherland, P. G., Uomoto, A., Wheeler, J. C., & Wills, B. J. 1983, *ApJ*, 270, 123
- Branch, D., Drucker, W., & Jeffery, D. J. 1988, *ApJ*, 330, L117
- Branch, D., & Tammann, G. A. 1992, *ARA&A*, 30, 359
- Branch, D., Fisher, A., & Nugent, P. 1993, *AJ*, 106, 2383
- Branch, D., Livio, M., Yungelson, L. R., Francesca, R. B., & Baron, E. 1995, *PASP*, 197, 1019
- Burstein, D., & Heiles, C. 1984, *ApJS*, 54, 33
- Cousins, A. W. J. 1981, *South African Astron. Obs. Circ.*, 6, 4
- de Vaucouleurs, G., et al. 1991, *Third Reference Catalogue of Bright Galaxies* (New York: Springer)
- Eder, J., Giovanelli, R., & Haynes, M. P. 1991, *AJ*, 102, 572
- Filippenko, A. V. 1997, *ARA&A*, 35, 309
- Filippenko, A. V., Porter, A. C., Sargent, W. L. W., & Schneider, D. P., 1986, *AJ*, 92, 1341
- Filippenko, A. V., et al. 1992a, *ApJ*, 384, L15
- . 1992b, *AJ*, 104, 1543 (F92)
- . 2000, *PASP*, in preparation
- Ford, C. H., et al. 1993, *AJ*, 106, 1101
- Garcia, A. M. 1993, *A&AS*, 100, 47
- Garnavich, P., Jha, S., & Kirshner, R. 1998, *IAU Circ.* 6980
- Hamuy, M., et al. 1994, *AJ*, 108, 2226
- Hamuy, M., Phillips, M. M., Suntzeff, N. B., Schommer, R. A., Maza, J., & Avilés, R. 1996a, *AJ*, 112, 2391
- Hamuy, M., Phillips, M. M., Suntzeff, N. B., Schommer, R. A., Maza, J., Smith, R. C., Lira, P., & Avilés, R. 1996b, *AJ*, 112, 2438
- Harkness, R. P., & Wheeler, J. C. 1990, in *Supernovae*, ed. A. G. Petschek (New York: Springer Verlag), p. 1
- Hillebrandt, W., & Niemeyer, J. C. 2000, *ARA&A*, in press
- Höflich, P., Khokhlov, A. M., & Wheeler, J. C. 1995, *ApJ*, 444, 831
- Höflich, P., & Khokhlov, A. M. 1996, *ApJ*, 457, 500
- Höflich, P., Khokhlov, A. M., & Wheeler, J. C., Phillips, M. M., Suntzeff, N. B., & Hamuy, M. 1996, *ApJ*, 472, L81
- Huchra, J. P., Vogeley, M. S., & Geller, M. J. 1999, *ApJS*, 121, 287
- Iben, I., Jr., & Tutukov, A. V. 1984, *ApJS*, 54, 335
- Ichikawa, T., & Fukugita, M. 1992, *ApJ*, 394, 61
- Jeffery, D. J., Leibundgut, B., Kirshner, R. P., Benetti, S., Branch, D., & Sonneborn, G. 1992, *ApJ*, 397, 304
- Jha, S., et al. 1999, *ApJS*, 125, 73
- Johnson, H. L., Mitchell, R. I., Iriarte, B., & Wisniewski, W. Z. 1966, *Commun. Lunar Planet. Lab.*, 4, 99
- Kirshner, R. P., et al. 1993, *ApJ*, 415, 589
- Khokhlov, A., Müller, E., & Höflich, P. 1993, *A&A*, 270, 223
- Kraan-Korteweg, R. C. 1986, *A&A Rev.*, 66, 255
- Landolt, A. U. 1992, *AJ*, 104, 340
- Leibundgut, B., & Pinto, P. A., 1992, *ApJ*, 401, L49
- Leibundgut, B., et al. 1993, *AJ*, 105, 301 (L93)
- Li, W. D., et al. 1999, *AJ*, 117, 2709
- Li, W. D., et al. 2000b, in *Cosmic Explosions*, eds. S. S. Holt and W. Zhang (New York: American Institute of Physics), p. 91
- Li, W. D., Filippenko, A. V., & Riess, A. G. 2000c, *ApJ*, submitted
- Li, W. D., Filippenko, A. V., Treffers, R. R., Riess, A. G., Hu, J., & Qiu, J. 2000d, *ApJ*, submitted
- Li, W. D., et al. 2001, in preparation
- Livio, M. 2000, in *Type Ia Supernovae: Theory and Cosmology* (Cambridge: Cambridge University Press), in press
- Livne, E. 1990, *ApJ*, 354, L53
- Mazzali, P. A., Chugai, N., Turatto, M., Lucy, L. B., Danziger, I. J., Cappellaro, E., Della Valle, M., & Benetti, S. 1997, *MNRAS*, 284, 151 (M97)
- Miller, J. S., & Stone, R. P. S. 1993, *Lick Obs. Tech. Rep.* 66 (Santa Cruz: Lick Obs.)
- Mochkovitch, R., & Livio, M. 1990, *A&A*, 236, 378
- Mochkovitch, R., Guerrero, J., & Segretain, L. 1997, in *Thermonuclear Supernovae*, eds. P. Ruiz-Lapuente, R. Canal, & J. Isern (Dordrecht: Kluwer), p. 187
- Modjaz, M., et al. 1998, *IAU Circ.* 6977
- Nomoto, K., Thielemann, F.-K., & Yokoi K. 1984, *ApJ*, 286, 644
- Nugent, P., Phillips, M., Baron, E., Branch, D., & Hauschildt, P. 1995, *ApJ*, 455, L147
- Oke, J. B., & Gunn, J. E. 1983, *ApJ*, 266, 713
- Pagel, B. E. J. 1997, *Nucleosynthesis and Chemical Evolution of Galaxies* (Cambridge: Cambridge University Press)
- Perlmutter, S., et al. 1997, *ApJ*, 483, 565
- . 1999, *ApJ*, 517, 565
- Phillips, M. M. 1993, *ApJ*, 413, L105
- Phillips, M. M., Wells, L. A., Suntzeff, N. B., Hamuy, M., Leibundgut, B., Kirshner, R. P., & Foltz, C. B. 1992, *AJ*, 103, 1632
- Phillips, M. M., et al. 1999, *AJ*, 118, 1766
- Richmond, M. W., Treffers, R. R., & Filippenko, A. V. 1993, *PASP*, 105, 1164
- Richmond, M. W., et al. 1995, *AJ*, 109, 2121
- Riess, A. G. 1999, in *Cosmic Flows Workshop*, eds. S. Courteau, M. Strauss, & J. Willick (Victoria, Canada: ASP series)
- Riess, A. G., Press, W. H., & Kirshner, R. P. 1995, *ApJ*, 445, L91
- . 1996, *ApJ*, 473, 88
- Riess, A. G., et al. 1998a, *AJ*, 116, 1009
- Riess, A. G., Nugent, P., Filippenko, A. V., Kirshner, R. P., & Perlmutter, S. 1998b, *ApJ*, 504, 935
- Riess, A. G., et al. 1999, *AJ*, 118, 2675
- Ruiz-Lapuente, P., Cappellaro, E., Turatto, M., Gouiffes, C., Danziger, I. J., della Valle, M., & Lucy, L. B. 1992, *ApJ*, 387, L33
- Ruiz-Lapuente, P., et al. 1993, *Nature*, 365, 728
- Ruiz-Lapuente, P., Kirshner, R. P., Phillips, M. M., Challis, P. M., Schmidt, B. P., Filippenko, A. V., & Wheeler, J. C. 1995, *ApJ*, 439, 60
- Saha, A., Sandage, A., Labhardt, L., Schwengeler, H., Tammann, G. A., Panagia, N., & Macchetto, F. D., 1995, *ApJ*, 438, 8
- Saio, H., & Nomoto, K. 1985, *A&A*, 150, L21
- . 1998, *ApJ*, 500, 388
- Savage, B. D., & Mathis, J. S. 1979, *ARA&A*, 17, 73
- Schlegel, D. J., Finkbeiner, D. P., & Davis, M. 1998, *ApJ*, 500, 525
- Schmidt, B. P., et al. 1993, *AJ*, 105, 2236
- . 1998, *ApJ*, 507, 46
- Stetson, P. B. 1987, *PASP*, 99, 191
- Tonry, J. L., Blakeslee, J. P., Ajhar, E. A., & Dressler, A. 2000, *ApJ*, 530, 625
- Treffers, R. R., Peng, C. Y., Filippenko, A. V., & Richmond, M. W. 1997, *IAU Circ.* 6627
- Turatto, M., et al. 1996, *MNRAS*, 283, 1 (T96)
- Turatto, M., Piemonte, A., Benetti, S., Cappellaro, E., Mazzali, P. A., Danziger, I. J., & Patat, F. 1998, *AJ*, 116, 2431
- Vaughan, T. E., Branch, D., Miller, D. L., & Perlmutter S. 1995, *ApJ*, 439, 558
- Vettolani, G., & Baiesi Pillastrini, G. C. 1987, *A&A*, 175, 9
- Wade, R. A., & Horne, K. 1988, *ApJ*, 324, 411
- Webbink, R. F. 1984, *ApJ*, 277, 355
- Wells, L. A., et al. 1994, *AJ*, 108, 2233
- Wheeler, J. C., & Harkness, R. P. 1990, *Rep. Prog. Phys.*, 53, 1467
- Woosley, S. E., & Weaver, T. A. 1986, *ARA&A*, 24, 205
- . 1994, *ApJ*, 423, 371
- Zehavi, I., Riess, A. G., Kirshner, R. P., & Dekel, A. 1998, *ApJ*, 503, 483